

The influence of the drag force on the safety domain

(A influência da força de arraste no domínio de proteção)

F. Pascoal¹, E.A. y Castro¹ and F.S.S. Rosa²

¹Faculdade de Ciências Integradas do Pontal, Universidade Federal de Uberlândia, Ituiutaba, MG, Brazil

²Laboratoire Charles Fabry, Institut d'Optique, Palaiseau Cedex, France

Recebido em 29/12/2010; Aceito em 23/2/2011; Publicado em 3/6/2011

In this work we compute the safety domain related to projectiles fired close to the Earth's surface, taking into account a linear (laminar regime) and a quadratic drag force (turbulent regime).

Keywords: projectile, safety domain, drag force.

Neste trabalho calcula-se o domínio de segurança relacionado ao lançamento de projéteis perto da superfície terrestre. Leva-se em consideração uma força de resistência proporcional à velocidade do projétil (regime laminar) e proporcional ao quadrado da velocidade (regime turbulento).

Palavras-chave: projéteis, domínio de proteção, força de arraste.

1. Introduction

The motion of projectiles under the influence of Earth's gravitational field is an extremely useful arena for students to exercise their knowledge of classical mechanics. This problem typically consists of a projectile fired with an arbitrary velocity and angle with respect to the Earth's surface, and from the appropriate initial data one should find a number of things like the horizontal range, time of flight and maximum height achieved by the projectile. In the simplest possible case, where the air resistance and Earth's curvature effects may be neglected, one can easily solve the equations for the projectile's trajectory in terms of the parabolic Galilean model and then discuss several aspects of the problem [1–3]. However, it is curious that just a few books and papers deal with an interesting feature of this problem, the parabola of safety [4–6].

Let us consider a concrete example in order to understand the concept of the parabola of safety. If a cannon fires projectiles with a certain maximum velocity in arbitrary directions, it is quite clear that there is only a finite volume V that these projectiles can explore, what naturally leads to the definition of the region *outside* this volume as a *safety zone*. In the case of a constant gravitational field, it is possible to show that the safety zone is separated from the “unsafe” zone by a paraboloid of revolution centered on the cannon [4–6], therefore known as the parabola of safety (Fig. 1).

While the safety zone is rarely considered in the lit-

¹E-mail: fabiopr@pontal.ufu.br.

erature even for the galilean case, we don't know of any attempt to evaluate it when the air resistance is taken into account. In this work, we intend to partially fill this gap by investigating the safety domain for spherical projects fired inside fluids in the laminar and turbulent regimes, in an effort to increase the amount of undergraduate-level material available when friction is relevant for the problem at hand.

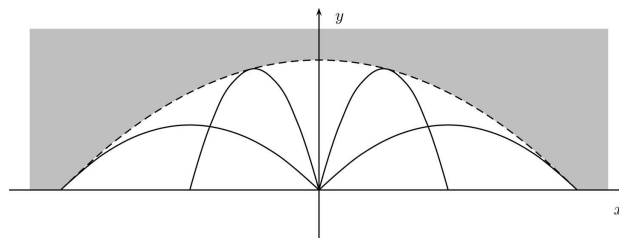


Figure 1 - Illustration of the safety domain. The solid lines represent some possible trajectories and the dashed line delimits the safety domain. If a projectile fired with initial speed v_0 , it can only reach a target in the white area.

2. The drag force and the Reynolds number

When a solid body moves through a fluid, the latter exerts forces on the surface of the former. A component called *drag force* imposes resistance to the body's

motion and is given phenomenologically by [1,7]

$$\mathbf{F}_D = -\frac{1}{2}C_D\rho A\mathbf{v}\mathbf{v}, \quad (1)$$

where ρ is the density of the fluid, A is the cross-sectional area perpendicular to the flow and \mathbf{v} respectively the velocity of the body (with $v = \sqrt{\mathbf{v} \cdot \mathbf{v}}$). The dimensionless drag coefficient C_D depends upon the viscosity η and density of the fluid, as well as upon the shape and velocity of the solid body.

It is natural to expect the drag force to depend on the type of *flow* around the object moving through the fluid. An extremely useful quantity for characterizing different types of flow is the *Reynolds number* [7,8], that in the case of a smooth sphere with radius r , may be defined as

$$Re = \frac{2r\rho v}{\eta}. \quad (2)$$

As an illustrative example, in Fig. 2 we plot the drag coefficient versus the Reynolds number for a smooth sphere [7,8]. Together with Eq.(1), it shows us that the drag force on a smooth sphere has a simple form in two different regimes: For small Reynolds numbers, the dashed line in Fig. 2 yields

$$C_D \simeq \frac{24}{Re} \Rightarrow \mathbf{F}_D \simeq -6\pi\eta r\mathbf{v}; \quad Re < 1, \quad (3)$$

while for intermediate Reynolds numbers, the dotted line gives

$$C_D \simeq 0.45 \Rightarrow \mathbf{F}_D \simeq -\frac{9}{4}\pi\rho r^2\mathbf{v}\mathbf{v}; \quad 10^3 < Re < 10^5. \quad (4)$$

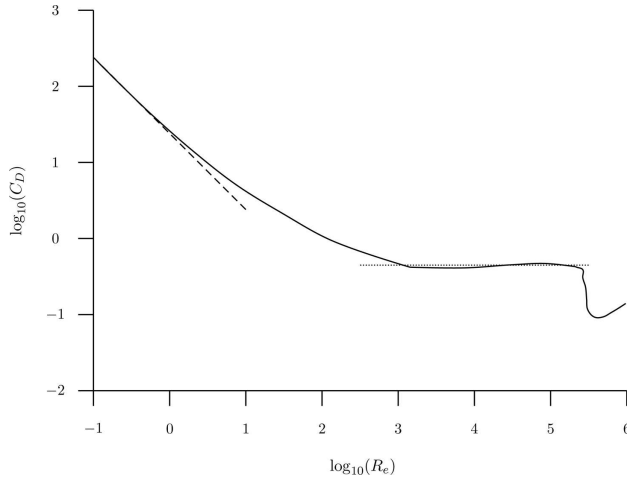


Figure 2 - Log-Log plot of experimental data of drag coefficient versus the Reynolds number for a smooth sphere.

Following the usual terminology in fluid mechanics, we denote by *laminar* the regime set by Eq. (3), *i.e.*, the one characterized by a drag force proportional to the speed, and by *turbulent* the regime one characterized by a quadratic law of resistance.²

²Technically, in this regime the flow is not entirely turbulent, since in the boundary layer the flow it is still laminar. However, as the wake is mainly turbulent at this point, we feel the jargon is adequate

3. The drag force and the deformation of the parabola of safety

In this section, we consider spherical projectiles characterized by a radius r and a mass m fired through a fluid with viscosity η and density ρ at the ground level. In addition, the projectiles are fired with a fixed speed v_0 but at an arbitrary elevation angle θ to the horizontal. We restrict our attention to the case where $v_0 \ll \sqrt{gR_E}$ (being R_E the Earth radius), so it is a good approximation to assume a constant gravitational field. A simple application of Newton's second law then gives the projectile's equations of motion

$$m\ddot{\mathbf{r}} = -mg\hat{z} + \mathbf{F}_D, \quad (5)$$

which is our starting point for the computation of the safety domain.

3.1. The laminar regime and the linear drag force

The laminar regime occurs when $Re < 1$ and, as we have seen, the drag force is approximately linear in the velocity. In that situation, we define s and z as the horizontal and vertical distances to the origin, in order to rewrite (5) as

$$\ddot{s} = -k_l\dot{s}; \quad (6)$$

$$\ddot{z} = -g - k_l\dot{z}, \quad (7)$$

where $k_l = 6\pi\eta r/m$. Given the initial conditions $\mathbf{r}(0) = 0$ and $\mathbf{v}(0) = v_0(\cos\theta\hat{s} + \sin\theta\hat{z})$, the solutions to the previous equations of motion are given by

$$s(t; \theta) = \frac{v_0}{k_l}(1 - e^{-k_l t})\cos\theta, \quad (8)$$

$$0 < t < t_{max},$$

$$z(t; \theta) = \frac{1}{k_l} \left(v_0 \sin\theta + \frac{g}{k_l} \right) \times (1 - e^{-k_l t}) - \frac{gt}{k_l}, \quad 0 < t < t_{max}, \quad (9)$$

where t_{max} is the (θ -dependent) time when the projectile hits the ground. By eliminating the time t in Eqs. (8) and (9), we obtain the path equation

$$z(s; \theta) = \left(\tan\theta + \frac{g}{k_l v_0 \cos\theta} \right) s + \frac{g}{k_l^2} \ln \left(1 - \frac{k_l s}{v_0 \cos\theta} \right). \quad (10)$$

Just as a consistency check, we can take the limit of small fluid resistance effect,

$$z(s; \theta) \simeq s \tan\theta - \frac{gs^2}{2v_0^2 \cos^2\theta} - \frac{k_l g s^3}{3v_0^3 \cos^3\theta}, \quad (11)$$

where it is clear that at zeroth order in k_l ($k_l t_{max} \ll 1$) we recover the parabolic Galilean solution [1–3].

In order to determine the safety zone, we have to calculate the envelope of all possible trajectories the projectiles may take. This can be done by evaluating the maximum vertical displacement $z(s, \theta)$ for a given horizontal displacement s , or, in other words, by finding all the points $p = (s, z(s, \Theta_s))$ that satisfy

$$\left. \frac{\partial z(s; \theta)}{\partial \theta} \right|_{\Theta_s} = 0. \quad (12)$$

Actually, the condition (12) only gives the condition for an extremum, which could be a minimum or a maximum. In this case, however, it follows at once from Eqs. (7) and (9) that

$$\ddot{z} = -e^{-k_l t} (g + k_l v_0 \sin \theta) < 0 \quad \forall t, \quad (13)$$

assuring that any occurring extremum is in fact a maximum.

In Fig. 3 we illustrate the procedure for a fixed horizontal distance $s = S$: from all possible trajectories, the one characterized by a inclination angle Θ_s is the one that gives the maximum vertical displacement $z(S, \Theta_s)$. Now, using the path Eq. (10) into Eq. (12) and dropping the subscript s from Θ_s , we obtain the horizontal coordinate of the surface delimiting the safety zone

$$S(\Theta) = \frac{v_0^2 \cos \Theta}{k_l v_0 + g \sin \Theta}. \quad (14)$$

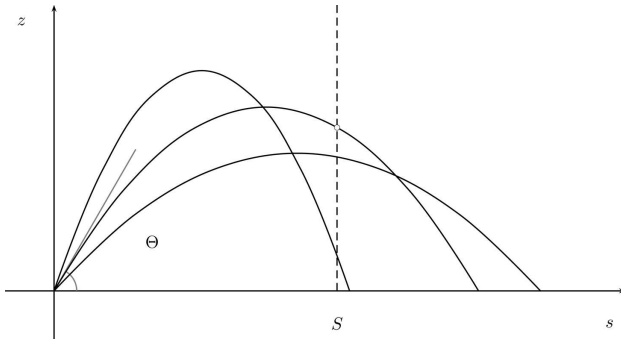


Figure 3 - By using equation (12), we are searching for the angle Θ that maximizes $Z(s, \theta)$.

By substituting Eq. (14) into Eq. (10), we get the vertical coordinate of that surface as a function of Θ

$$Z(\Theta) = \frac{k_l v_0^2 \sin \Theta + g v_0}{k_l^2 v_0 + k_l g \sin \Theta} - \frac{g}{k_l^2} \ln \left(1 + \frac{k_l v_0}{g \sin \Theta} \right). \quad (15)$$

Given that $\sin \Theta$ is in principle unknown, we have to eliminate it from the previous equation in order to get an explicit expression for the boundary of the safety domain. This can be done by manipulating Eq. (14) to obtain

$$(S^2 g^2 + v_0^4) \sin^2 \Theta + 2S^2 k_l v_0 g \sin \Theta + S^2 k_l^2 v_0^2 - v_0^4 = 0 \quad (16)$$

and therefore

$$\sin \Theta = -\frac{S^2 k_l v_0 g}{S^2 g^2 + v_0^4} + \frac{v_0^2 \sqrt{(g^2 - k_l^2 v_0^2) S^2 + v_0^4}}{S^2 g^2 + v_0^4}. \quad (17)$$

Inserting Eq. (17) into Eq. (15) and consequently eliminating $\sin \Theta$, we obtain the analytical expression

$$Z(S) = \frac{v_0^2}{g} + \frac{(g^2 S^2 + v_0^4) (g^2 - k_l^2 v_0^2)}{k_l g^2 v_0 \sqrt{(g^2 - k_l^2 v_0^2) S^2 + v_0^4} + k_l^2 g v_0^4} + \frac{g}{k_l^2} \ln \left(\frac{g v_0 \sqrt{(g^2 - k_l^2 v_0^2) S^2 + v_0^4} - k_l g^2 S^2}{g v_0 \sqrt{(g^2 - k_l^2 v_0^2) S^2 + v_0^4} + k_l v_0^4} \right). \quad (18)$$

The region above that surface represents the safety domain when a drag force linear in the velocity is considered. In Fig. 4, we plot the surface that delimits the safety domain for some different values of $\xi_l = k_l v_0 / g$. As expected, the safety domain increases as the fluid resistance effects becomes more relevant, *i.e.*, as ξ_l increases. Expanding Eq. (18) for small values of $k_l v_0 / g$, we obtain

$$Z(S) \simeq \frac{1}{2} \left(\frac{v_0^2}{g} - \frac{g S^2}{v_0^2} \right) - \frac{k_l}{3g^2 v_0^3} (g^2 S^2 + v_0^4)^{3/2}, \quad (19)$$

from where it is clear that we obtain the parabola of safety in the limit of no fluid resistance [4–6].

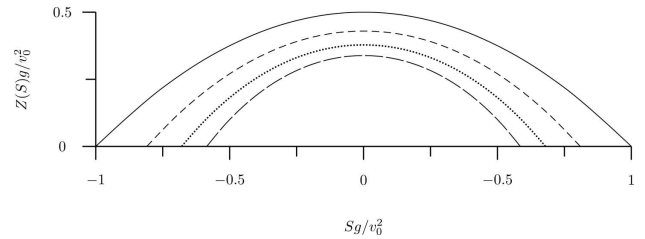


Figure 4 - Plots of the envelope of all the possible trajectories with different values of ξ_l . The solid line represents $\xi_l = 0$ (the case without the fluid resistance effect), the dashed, the dotted and the discontinuous line represents $\xi_l = 0.25$, $\xi_l = 0.5$ and $\xi_l = 0.75$, respectively.

In addition, we may also obtain the time T when a projectile fired with an elevation Θ reaches the envelope. A simple substitution of Eq. (14) into Eq. (8) and subsequent isolation of t quickly yields

$$T = \frac{1}{k_l} \ln \left(\frac{k_l v_0}{g \sin \Theta} + 1 \right), \quad (20)$$

but this is not quite the complete story: the previous equation makes sense only if $T < t_{max}$, the latter given implicitly by the non-zero solution of $z(t, \Theta) = 0$. Bearing that in mind, from Eqs. (9) and (20) it is straightforward to get the z -component of the velocity at the time T

$$\dot{Z}(T; \Theta) = -\frac{v_0 g \cos^2 \Theta}{k_l v_0 + g \sin \Theta}. \quad (21)$$

Given that all quantities on the previous expression are positive we conclude that $\dot{Z}(T; \Theta) \leq 0$ always, and therefore that the projectile always touch the surface that delimits the safety domain after it reaches the highest point.

3.2. The turbulent regime and the quadratic drag force

In the turbulent regime, the drag force is quadratic in the speed and then Newton's second law becomes

$$\ddot{s} = -k_q \sqrt{\dot{s}^2 + \dot{z}^2} \dot{s}; \quad (22)$$

$$\ddot{z} = -g - k_q \sqrt{\dot{s}^2 + \dot{z}^2} \dot{z}, \quad (23)$$

where now $k_q \simeq 9\pi\rho r^2/(4m)$. Equations (22) and (23) are a set of non-linear coupled differential equations and unfortunately not amenable to simple analytical procedures, which means that a numerical analysis is needed to continue our study.

In Fig. 5, we plot the trajectory with $\theta = \pi/4$ for different values of $\xi_q = k_q v_0^2/g$. As we can see, the drag force can have a dramatic effect on the projectiles motion.

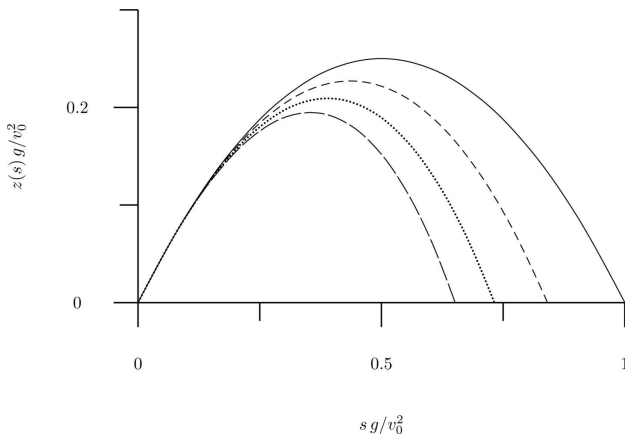


Figure 5 - Plots of the trajectories for different values of $\xi_q = k_q v_0^2/g$. The solid line represents $\xi_q = 0$ (the case without the fluid resistance effect), the dashed, the dotted and the discontinuous line represents $\xi_q = 0.25$, $\xi_q = 0.5$ and $\xi_q = 0.75$, respectively. The elevation angle was fixed in $\pi/4$.

In order to analyze the behavior of the safety domain, we used the same idea of Eq. (12), we made a short computational routine that searches for the value of the elevation angle θ that maximizes the function $z(s, \theta)$ for a fixed value $s = S$ on the horizontal coordinate. In Fig. 6, we plot our results. As expected, the safety domain increases while the while ξ_l increases.

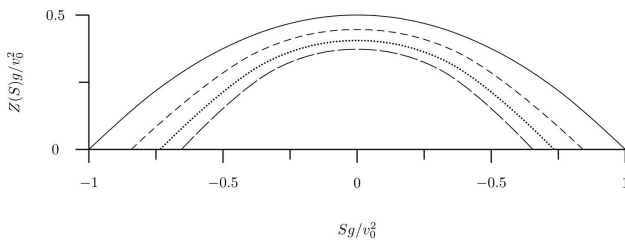


Figure 6 - Plots of the envelope of the safety domain for different values of ξ_q (Same patterns used in Fig. 5).

In Fig. 7, we plot the z component of the velocity when the projectile reaches the envelope of the safety

domain. As in the laminar regime, in the turbulent regime, the projectile always reaches the envelope when it is falling.

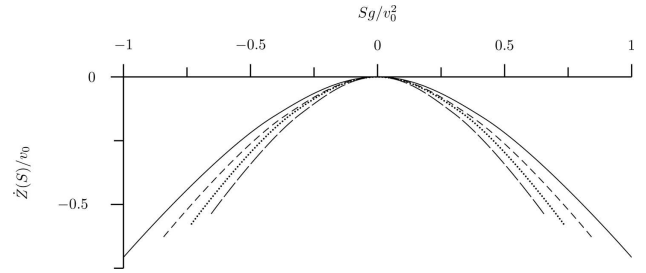


Figure 7 - Plots of the vertical component of the velocity \dot{z} when the projectile reaches the envelope of the safety domain as a function of the horizontal component S for different values of ξ_q (Same patterns used in Fig. 5).

4. Final remarks

We obtained an exact analytical expression for the safety domain in the laminar regime, which is a good approximation when $R_e < 1$. An interesting example where such condition is satisfied consists on a small projectile fired though a high viscous medium (like glycerine, honey or glucose) with a small initial speed. The turbulent regime with a quadratic drag force does not have an analytical solution, but since that it describes very well the extremely relevant case of the motion of a cannonball fired in air, we solved it numerically in order to analyze its safety domain as well.

5. Acknowledgments

The authors would like to thank C. Farina and A.J. Chiquito for valuable comments.

Referências

- [1] J.B. Marion and S.T. Thornton, *Classical Dynamics of Particles and Systems* (Brooks Cole, Belmont, 2004).
- [2] H. Goldstein, C.P. Poole and J.L. Safko, *Classical Mechanics* (Addison Wesley, Boston, 1980).
- [3] K.R. Symon, *Mechanics* (Addison Wesley, Boston, 1971).
- [4] Pierre Lucie, *Am. J. Phys.* **47**, 2 (1979).
- [5] Tai L. Show, *Classical Mechanics* (John Wiley & Sons, New York, 1995).
- [6] J.-M. Richard, *Eur. J. Phys.* **25**, 835 (2004).
- [7] L.D. Landau and E.M. Lifshitz, *Fluid Mechanics* (Butterworth-Heinemann, Oxford, 1987).
- [8] R.W. Fox and A.L. McDonald, *Introduction to Fluid Mechanics* (John Wiley & Sons, Inc., New York, 1978), 2^a ed.